Inorganic Chemistry
Cite This: Inorg. Chem. 2019, 58, 12798−12808
Article
pubs.acs.org/IC

Comparison of MRI Properties between Multimeric DOTAGA and DO3A Gadolinium-Dendron Conjugates

Maleotane Ndiaye,[†,⊥] Volodymyr Malytskyi,[‡,⊥] Thomas Vangijzegem,[†] Félix Sauvage,[∥] Mike Wels,[∥] Cyril Cadiou,[‡] Juliette Moreau,[‡] Céline Henoumont,[†] Sébastien Boutry,[§] Robert N. Muller,[†,§] Dominique Harakat,[‡] Stefaan De Smedt,[∥] Sophie Laurent,*[,†,§] and Françoise Chuburu*[,‡]

[†]Laboratoire de RMN et d'Imagerie Moléculaire, Université de Mons, B-7000 Mons, Belgium

[‡]Institut de Chimie Moléculaire de Reims, CNRS UMR 7312, Université de Reims Champagne-Ardenne URCA, F-51685 Reims Cedex 2, France

[§]Center for Microscopy and Molecular Imaging, Rue Adrienne Bolland 8, B-6041 Charleroi, Belgium

[∥]Laboratory of General Biochemistry and Physical Pharmacy, Ghent University, Ottergemsesteenweg 460, 9000 Ghent, Belgium

Supporting Information

ABSTRACT: The inherent lack of sensitivity of MRI needs the development of new Gd contrast agents in order to extend the application of this technique to cellular imaging. For this purpose, two multimeric MR contrast agents obtained by peptidic coupling between an amido amine dendron and GdDOTAGA chelates (premetalation strategy, G1-4GdDOTAGA) or DO3A derivatives which then were postmetalated (G1-4GdDO3A) have been prepared. By comparison to the monomers, an increase of longitudinal relaxivity has been observed for both structures. Especially for G1-4GdDO3A, a marked increase is observed between 20 and 60 MHz. This structure differs from G1-4GdDOTAGA by an increased rigidity due to the aromatic linker between each chelate and the organic framework. This has the effect of limiting local rotational movements, which has a positive impact on relaxivity.

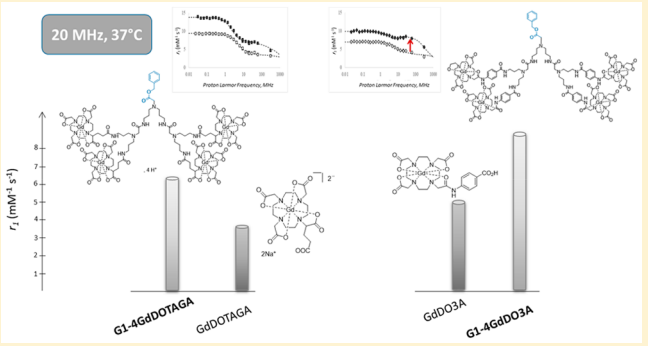

INTRODUCTION

Due to its high spatial and temporal resolutions, magnetic resonance imaging (MRI) is a mainstream method for clinical diagnosis and therapeutic decision-making. The MRI signals arise from the ^{1}H abundancy in the body. When the body is exposed to a strong magnetic field, the ^{1}H nuclei, which are magnetically active, orient themselves within this magnetic field. When the body is then submitted to radiofrequency pulses, the energy as well as the orientation of the nuclei change and as they relax to their initial states, a resonance radio-wave is emitted. The recovery of this MRI signal and its spatial encoding leads to image production.[1] In MRI, the main contrast parameters are ^{1}H density, longitudinal T_1, and transversal T_2 proton relaxation times. Although T_1 and T_2 are generally reduced in injured tissues, there is considerable overlap of relaxation times between healthy and injured damaged tissues on native MRI. This stresses the need for MRI contrast agent injection to enhance the contrast.

Paramagnetic contrast agents are known to exert a strong stimulation to T_1 relaxation, and gadolinium-based contrast agents (GBCAs) are ideal candidates for producing MRI contrastophores that affect T_1 of water protons in tissues.[2] The MRI effectiveness of GBCAs is evaluated from their longitudinal r_1 relaxivity value, which refers to the increase in the inverse of T_1 per millimolar metal ion. The GBCAs efficacy to affect the relaxation of protons in tissues is related to several parameters such as its molecular rotational correlation time τ_R, the number of inner-sphere water molecules q, or the exchange rate of these inner-sphere water molecules (k_{ex}).[2,3] Low molecular weight GBCAs are the active substances of the commercially and clinically available MRI contrast agents.[4] Their low molecular weight favors their rapid elimination from the body through the renal pathway, which effectively avoids deleterious side effects associated with gadolinium (Gd) body accumulation (*e.g.* nephrogenic systemic fibrosis (NSF)).[5] Moreover, the relaxivity of small GBCAs is limited by their rapid tumbling motions which results in a fast rotational correlation time τ_R ($\sim 10^{-10}$ s) and then a low relaxivity between 20 and 60 MHz (3−5 mM^{-1} s^{-1}).

In order to amplify the MRI efficacy, the conjugation of small GBCAs with macromolecular carriers has been investigated.[2,3,6] Among them, dendrimers and particularly polyamidoamines (PAMAM) have been explored because of their more rigid structure,[7] and GBCA conjugation with PAMAM dendrimers of different generations was carried out.[8]

Received: June 12, 2019
Published: September 9, 2019

DOI: 10.1021/acs.inorgchem.9b01747
Inorg. Chem. 2019, 58, 12798−12808

Scheme 1. Structure of the Multimeric Systems Investigated Herein

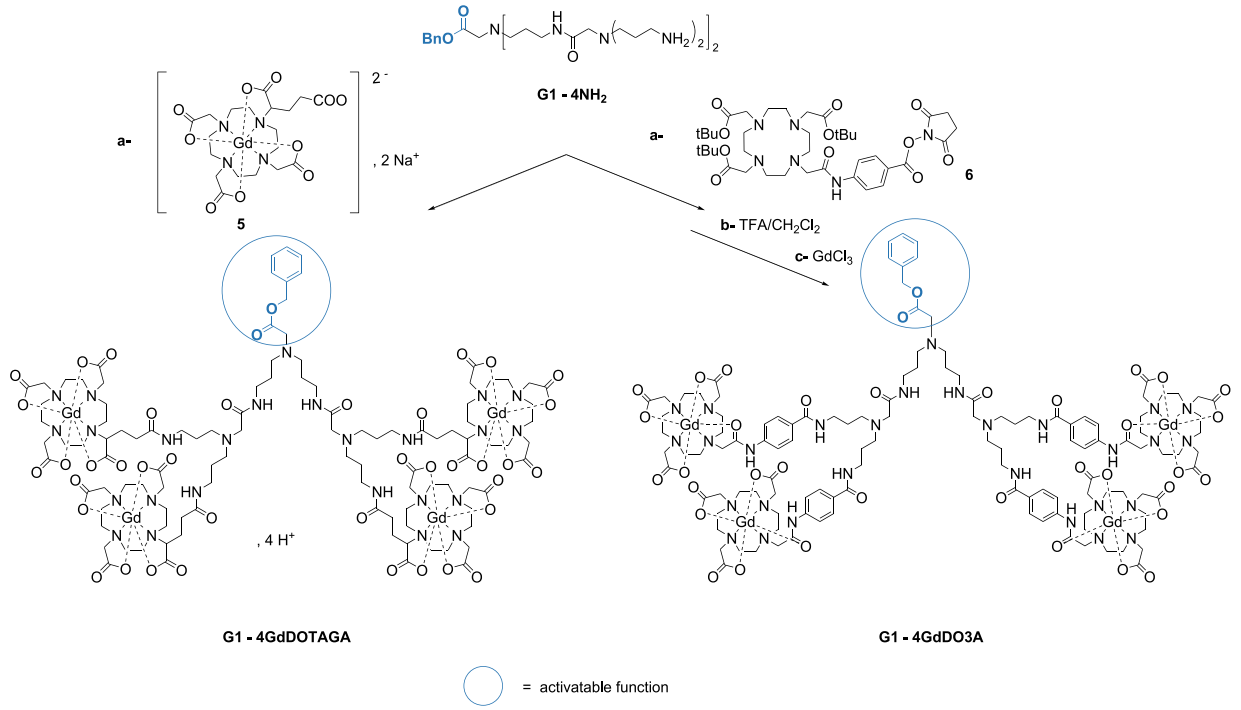

As the result of the reduced rotational tumbling rate ($1/\tau_R$), the proton relaxivity was improved at intermediate fields, but the efficiency of dendrimeric GBCAs did not show a linear dependence with their molecular mass. Besides, the enhancement clearly tends to diminish for larger systems. Moreover, high-generation dendrimers are not easy to prepare and to purify,[8] and a latent cytotoxicity is observed due to a slow degradation *in vivo*.[9]

In this report, we propose to take advantage of the dendronization strategy to design multimeric GBCAs. The dendritic structures prepared in this work (Scheme 1) rely on a common bifunctional amido amine core (G1-4NH_2). The installation of MRI contrastophores will herein be carried out by peptidic coupling with the amino groups of the G1-4NH_2 core. On the resulting **G1-4GdDOTAGA** and **G1-4GdDO3A** structures, there will remain an activatable group (benzyl ester group), which may be released in the future, in order to introduce either a targeting ligand or a second imaging probe. Indeed, in order to reduce ambiguities in the MRI signal analysis, it will be interesting to develop contrast agents able to multiplex an MRI probe to a more sensitive one (for instance an optical imaging probe),[10] provided that differences in concentration imposed by differences in sensitivity are taken into account in the system design.

Two different approaches were used to obtain the desired multimeric structures. For the first one, **G1-4GdDOTAGA**, four premetalated GdDOTAGA chelates were grafted on the central G1-4NH_2 core. The second one **G1-4GdDO3A**, was obtained by covalent linking of four DO3A macrocyclic units on the same central G1-4NH_2 core, followed by Gd metalation. In order to ensure a good thermodynamic stability of the corresponding metal complexes, these two structures were designed on the basis of macrocyclic GBCAs, and their synthesis is described in the paper. Before considering any additional functionalization of these multimeric GBCAs, we have evaluated their respective efficacy to enhance MRI sensitivity as well as their kinetic inertness. Finally, their harmlessness toward fibroblasts was investigated.

EXPERIMENTAL SECTION

All reagents were purchased from commercial suppliers and used without further purification. ^{1}H NMR and ^{13}C NMR spectra were recorded on a 600 MHz Bruker Avance III spectrometer equipped with a TCI cryoprobe and on a Bruker Avance Neo 600 MHz. The chemical shifts were reported in parts per million (δ scale). Traces of residual solvents were used as internal standards for ^{1}H and ^{13}C chemical shift referencing. Abbreviations: s: singlet, d: doublet, t: triplet, q: quadruplet, m: multiplet, ws: wide signal.

FTIR absorption spectra were obtained on a Thermo Scientific Nicolet iS5 spectrometer equipped with ATR iD5 accessory, and wavenumbers are reported in cm^{-1}.

All mass spectra were collected by using a SYNAPT G2-Si HDMS (Waters Corp., Manchester, UK) equipped with an electrospray ionization source. ESI mass spectra were acquired over the m/z 100−4000 range. The desolvation gas was set to 800 L·h^{-1} at a temperature of 200 °C, the cone gas was set to 40 L·h^{-1}, and the source temperature was set to 120 °C. The capillary voltage was set to 2500 V. Spectra were acquired in continuum and negative mode.

Column chromatographies were performed using silica gel (230−400 mesh) (Macherey-Nagel GmbH, Germany). Inversed phase chromatography was performed on C18 bonded silica (45−75 μm, VersaFlash). The excess of Gd^{3+} ions was removed on Chelex 100 sodium form resin (50−100 mesh, purchased from Sigma).

Syntheses. The syntheses of starting dendrimer **G1-4NH_2**, DO3A-based ligand in the form of activated ester **DO3A(*t*Bu)$_3$NHS**, as well as mononuclear complexes **GdDOTAGA** and **GdDO3A-COOH** were performed as described in the Supporting Information (SI 1, 2, Supporting Information).

G1-4GdDOTAGA Synthesis. The **G1-4NH_2** dendrimer (200 mg, 0.20 mmol, 1 equiv) and Gd-chelate **Na_2GdDOTAGA 5** (84% purity (SI 2, Supporting Information) 955 mg, 1.19 mmol, 6 equiv) were loaded into a flask flashed with argon. Anhydrous DMSO (50 mL) and triethylamine (166 μL, 1.19 mmol, 6 equiv) were added, and the mixture was homogenized in ultrasonic bath.

After addition of 1-[bis(dimethylamino)methylene]-1H-1,2,3-triazolo[4,5-*b*]pyridinium3-oxidhexafluorophosphate (HATU, 452

DOI: 10.1021/acs.inorgchem.9b01747
Inorg. Chem. 2019, 58, 12798−12808

mg, 1.19 mmol, 6 equiv), the mixture was stirred at room temperature for 1 day. Addition of ethyl acetate (450 mL) provoked the formation of a precipitate that was recovered and washed two times with ethyl acetate (30 mL). The precipitate was taken up with 10 mL of distilled water; the resulting solution was split into two, diluted to 12 mL with water and loaded into two Vivaspin 15R tubes (MWCO 2000 g/mol) for ultrafiltration (6000 g for 45 min). Three ultrafiltration cycles were performed afterward; the remaining solutions were transferred into a round-bottom flask and evaporated under reduced pressure to afford **G1-4GdDOTAGA** (499 mg, Gd-purity found by relaxometric study 89%, 0.14 mmol, yield 73%) as a crystalline solid. The absence of free gadolinium ions was checked by a colorimetric test with xylenol orange as a dye.[11] FTIR: 1595 cm^{-1}. HR-MS (ESI): m/z calculated for $[M - H]^-$: 3071.8726/found: 3071.8738; calculated for $[M - 2H]^{2-}$: 1535.4324/found: 1535.4336 (values are given for the highest component of isotopic profile; $M \equiv C_{107}H_{167}Gd_4N_{25}O_{40}$). Detailed HRMS spectra with simulated isotopic distribution profiles are given in SI 3, Supporting Information.

G1-4GdDO3A Synthesis. *G1-4[DO3A(tBu)$_3$].* To a solution of **G1-4NH$_2$** dendrimer (0.411 g, 0.42 mmol, 1 equiv) in DMF (5 mL) and DIPEA (0.99 mL, 5.83 mmol, 14 equiv) was added the solution of the activated ester **6** (2.112 g, 2.67 mmol, 6.3 equiv, prepared as described in SI 4, Supporting Information) in dichloromethane (5 mL), and the mixture was stirred for 48 h under a nitrogen atmosphere at room temperature. The solution was diluted with ethyl acetate (15 mL) and extracted three times with distilled water (3 × 30 mL) and brine (3 × 30 mL). Organic phase was dried over sodium sulfate, filtered, and concentrated under reduced pressure. A white solid was isolated (0.48 g) containing the desired compound as revealed by mass spectrometry. It was used in the further synthetic step without purification.

HR-MS (ESI): m/z calculated for $[C_{171}H_{279}N_{29}O_{36}+Cl]^-$: 3351.0620/found: 3351.0625.

G1-4DO3A. The compound **G1-4[DO3A(tBu)$_3$]** (0.48 g) was dissolved in a mixture of dichloromethane and trifluoroacetic acid (20 mL, 1:1 v/v), and this solution was stirred at room temperature for 48 h. The reaction mixture was concentrated under reduced pressure, and the residue precipitated in diethyl ether and washed three times with this solvent (3 × 30 mL). The obtained product was solubilized in distilled water (10 mL) and purified by dialysis (dialysis membrane MWCO 500−1000 Da, VWR) against 1 L of distilled water (which was changed four times, after 2.5, 6.5, 11.5, and 18 h). After dialysis, the resulting solution was freeze-dried and the desired dendron **G1-4DO3A** obtained (0.40 g, 0.15 mmol, yield 36% over two steps from **G1-4NH$_2$**).

^{1}H NMR (600.16 MHz, DMSO-d_6, 25 °C): δ 1.81 (ws, 4H, -NHCH$_2$C$\underline{H}_2$CH$_2$$\underline{N}$<), 1.90 (ws, NHCH$_2C\underline{H}_2CH_2$$\underline{N}$<), 2.8−5.4 (ws, dendrimer CH$_2$ and cyclen CH$_2$), 3.60 (s, 2H, >NC$\underline{H}_2$COOBn), 5.21 (s, 2H, −COOC$\underline{H}_2$Ph), 7.32−7.44 (m, 5H, C$\underline{H}$), 7.66 (d, 8H, ^3J = 8.4 Hz, C$\underline{H}$), 7.83 (d, 8H, ^3J = 8.4 Hz, C$\underline{H}$), 8.63 (s, 4H, N$\underline{H}$), 8.86 (s, 2H, N$\underline{H}$) 10.78 (ws, 4H, N$\underline{H}$).

^{13}C NMR (150.9 MHz, DMSO-d_6, 25 °C): δ 24.03, 26.81, 28.27, 36.35, 36.53, 51.40, 51.51, 51.74, 52.35, 53.11, 53.47, 54.91, 55.05, 113.54, 115.51, 117.47, 118.58, 119.00, 119.43, 128.19, 128.45, 128.54, 129.15, 130.82, 141.09, 157.87, 158.09, 158.32, 158.54, 163.66, 164.60, 165.93. FTIR: 1733 cm^{-1}, 1669 cm^{-1}.

HR-MS (ESI): m/z calculated for $[C_{123}H_{183}N_{29}O_{36}-H]^-$: 2642.3333/found: 2642.3303; calculated for $[C_{123}H_{183}N_{29}O_{36}-2H]^{2-}$: 1320.6627/found: 1320.6633.

G1-4GdDO3A. The dendron **G1-4DO3A** (0.40g, 0.15 mmol, 1 equiv) was dissolved in distilled water (2.5 mL), and the pH of the corresponding solution was adjusted to 5.5 with 1 M solution of sodium hydroxide. Gadolinium chloride ($GdCl_3 \cdot 6H_2O$, 0.34 g, 0.91 mmol, 6 equiv) was dissolved in distilled water (10 mL) and added to the solution of dendron **G1-4DO3A**. The pH of the mixture was adjusted again to 5.5, and the reaction mixture was stirred at room temperature for 1 day. The solution was treated for 1 h with Chelex 100 resin to remove the excess of gadolinium ions (in **G1-4GdDO3A** sample, the absence of free gadolinium ions was checked as previously, by complexometry with xylenol orange as a dye).[11] The resin was separated by centrifugation and the solution was concentrated under reduced pressure. The resulting crude product was dissolved in water (10 mL) and purified by dialysis (membrane with MWCO 500−1000 Da, VWR) against 1 L of distilled water (which was changed after 2.5, 6.5, 11.5, and 18 h). The dialyzed solution was freeze-dried leading to **G1-4GdDO3A** (0.12 g, 0.038 mmol, yield 25%). FTIR: 1600 cm^{-1}. HR-MS (ESI): m/z calculated for $[M - H]^-$: 3259.9368/found: 3259.9368; calculated for $[M - 2H]^{2-}$: 1629.4645/found: 1629.4651 (values are given for the highest component of isotopic profile; $M \equiv C_{123}H_{171}Gd_4N_{29}O_{36}$). Detailed HRMS spectra with simulated isotopic distribution profiles are given in SI 5, Supporting Information.

Determination of Gd Concentration for Relaxometric Measurements. To determine Gd^{3+} concentration, either ICP-OES or relaxometric measurements were performed. Previously, the absence of free Gd^{3+} ion in the analyzed samples was checked by complexometry with xylenol orange as a dye.[11] Furthermore, each sample (200 μL) was submitted to an acidic digestion (H_2O/HNO_3 1:1 v/v, 200 μL) to release Gd^{3+}. For ICP-OES measurements, volumetric dilutions were carried out to achieve an appropriate Gd concentration within the working range of the method. Samples were analyzed using a Varian Liberty Series II spectrometer. Counts of Gd were correlated to a Gd calibration curve generated by mixing $Gd(NO_3)_3$ standard prepared under the same acidic conditions. For relaxometry measurements, the longitudinal relaxation rate of the digested acidic solution was then determined after subtraction of the diamagnetic contribution (0.35 s^{-1} at 37 °C for the H_2O/HNO_3 1:1 v/v solution). This value was compared to the one of a 1 mM $GdCl_3$ solution (11.76 s^{-1}), and after taking into account the dilution factor (2), the Gd^{3+} concentration was obtained for the sample of interest. Both methods gave similar results since for a solution of **G1-4GdDOTAGA**, a Gd concentration of 1.68 mM was found by ICP-OES while the same solution analyzed by relaxometry gave a concentration of 1.63 mM. Similar results were obtained for a **G1-4GdDO3A** solution, i.e. 1.51 mM and 1.54 mM in Gd by ICP-OES and relaxometry respectively (between 2 and 3% error between the two methods). For determination of r_1 relaxivities Gd concentration determined by relaxometry was used.

Relaxometric Measurements. *T_1 Measurements at 20 MHz (0.47 T).* T_1 measurements were performed in water on a Bruker mq20 minispec relaxometer (0.47 T) using an inversion recovery pulse sequence. The measurements were performed at nine different temperatures between 5 and 45 °C. The temperature was equilibrated before each scan. The inverse of the paramagnetic longitudinal relaxation time ($1/T_{1para}$, s^{-1}) of each sample was calculated according to

$$(1/T_{1para}) = (1/T_{1observed}) - (1/T_{1dia})$$

$1/T_{1para}$ values were divided by Gd^{3+} concentration (mM) to determine **G1-4GdDOTAGA** and **G1-4GdDO3A** relaxivities r_1 (s^{-1} mM^{-1}).

NMRD Profiles. ^{1}H NMRD profiles were measured on a Stelar Spinmaster FFC fast field cycling NMR relaxometer (Stelar, Mede, Pavia, Italy) over a range of magnetic fields extending from 0.24 mT to 0.7 T (which corresponds to ^{1}H Larmor frequencies from 0.01 to 30 MHz) using 0.5 mL samples in 7.5 mm o.d. tubes. The temperature was kept constant at 37 °C. Additional relaxation rates at 60 and 300 MHz were obtained with Bruker Minispec mq60 and Bruker Avance-300 MHz spectrometers, respectively (Bruker, Karlsruhe, Germany). The least-squares fitting of the ^{1}H NMRD data was performed using a homemade program (Fitting2000) and equations from the Solomon and Bloembergen (SBM) theory for the small gadolinium complexes or from the Lipari-Szabo theory for the slow rotating macromolecular contrast agents. In the fitting procedure, the r_{GdH} distance was fixed to 3.10 Å and the closest approach of the bulk water protons to the Gd^{3+} ion, d_{GdH}, to 3.6 Å.[12] The diffusion constant D has been fixed to 3.0 × 10^{-9} m^2 s^{-1},[13] and the hydration number q was 1, as determined by luminescence lifetime measurements on the Eu^{3+} analogues (SI 6, Supporting Information). The water exchange rate $k_{ex} = 1/\tau_m$ where τ_m is the

DOI: 10.1021/acs.inorgchem.9b01747
Inorg. Chem. 2019, 58, 12798−12808

Table 1. Best-Fit Parameters Obtained from the Fitting of the ^{1}H NMRD Profiles to the SBM Theory, Including the Lipari–Szabo Approach for Internal Flexibility[a]

	d (nm)[b]	r (nm)[b]	τ_M (ns)[c]	q[b]	τ_{SO} (ps)	τ_V (ps)	τ_{RG} (ps)	τ_{RL} (ps)	S^2
G1-4GdDOTAGA	0.36	0.31	97	1	332 ± 11	31.1 ± 4.3	700 ± 112	150.0 ± 0.9	0.051 ± 0.015
G1-4GdDO3A	0.36	0.31	505	1	126 ± 3	37.4 ± 1.8	800 ± 94	167 ± 13	0.20 ± 0.02

[a]The definition of the parameters is given in the Experimental Section. [b]Fixed parameters. [c]Value obtained from ^{17}O experiments.

Scheme 2. Synthesis of G1-4NH$_2$ Dendron

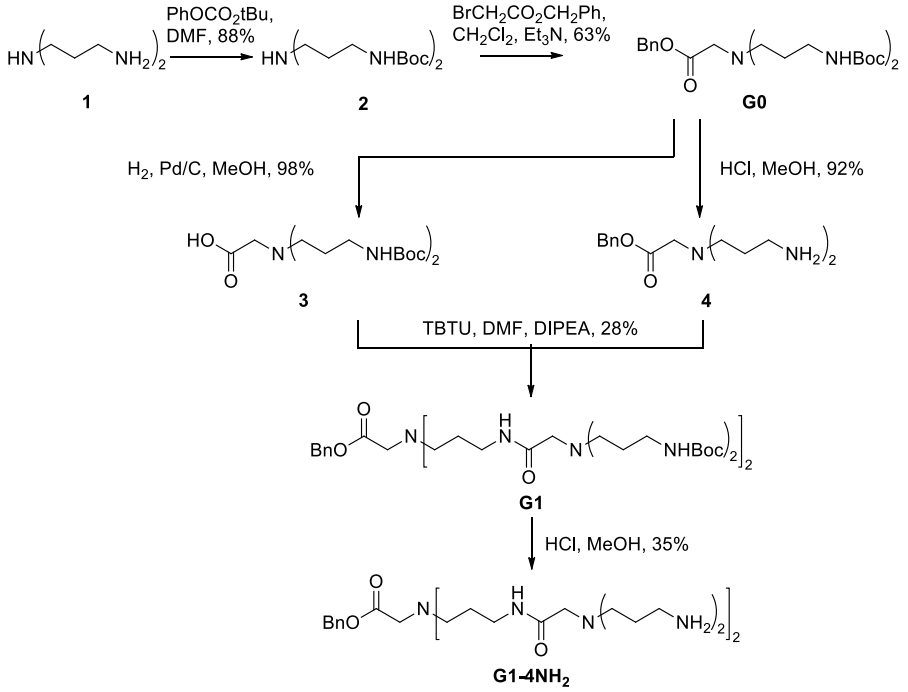

residence time of the coordinated water molecule in the inner sphere, was fixed to the value obtained by independent ^{17}O measurements of the transverse relaxation time of water $(1/T_2)$ according to the temperature. The fitting procedure allowed the determination of τ_{SO}, the gadolinium electronic relaxation time at zero field, τ_V, the correlation time that modulates the electronic relaxation, and τ_R, the rotational correlation time (if the SBM theory is used), or τ_{RG} and τ_{RL}, *i.e.* the rotational correlation times describing the global and local motions, respectively, and S^2 that reflect the degree of spatial restriction of the local motion with respect to the global motion ($0 \leq S^2 \leq 1$,$S^2 = 0$ for isotropic internal motions, $S^2 = 1$ for completely restricted internal motions), if the Lipari–Szabo approach is used. The best-fit parameters obtained from the analysis of ^{1}H NMRD data are summarized in Table 1.

Temperature Dependent ^{17}O NMR Measurements. The transverse ^{17}O relaxation rates $(1/T_2)$ were measured in aqueous solutions of **G1-4GdDOTAGA** and **G1-4GdDO3A** (12 mM) in the temperature range 7–77 °C, on a Bruker Avance 500 (11.7 T, 67.8 MHz) spectrometer. The temperature was calculated according to a previous calibration with ethylene glycol and methanol. Proton decoupling was applied during all the acquisitions. Transverse relaxation times (T_2) were obtained by the measurement of the signal width at midheight. The data are presented as the reduced transverse relaxation rate $1/T_2^R = 55.55/([Gd_{complex}]\cdot q\cdot T_2^P)$, where $[Gd_{complex}]$ is the molar concentration of the complex, q is the number of coordinated water molecules, and T_2^P is the paramagnetic transverse relaxation rate obtained after subtraction of the diamagnetic contribution from the observed relaxation rate. The treatment of the experimental data was performed as described elsewhere.[14] The following parameters were determined: $A/\hbar$, the hyperfine coupling constant between the oxygen nucleus of the bound water molecule and the Gd^{3+} ion; τ_v, the correlation time modulating the electronic relaxation of Gd^{3+}; E_v, the activation energy related to τ_v; B, related to the mean-square of the zero field splitting energy Δ ($B = 2.4\Delta^2$); and $\Delta H^{\ddagger}$ and $\Delta S^{\ddagger}$ the enthalpy and entropy of activation, respectively, of the water exchange process. The number of coordinated water molecules was set to 1.

T1-Weighted Images. MR imaging of **G1-4GdDOTAGA** and **G1-4GdDO3A** were performed using a 1.0 T MRI device (ICON, Bruker) using a T1-weighted spin–echo sequence (TR = 300 ms, TE = 12 ms, resolution = 208 × 195 μm, slice thickness = 1.25 mm, 4 averages). Solutions of **G1-4GdDOTAGA** and **G1-4GdDO3A** were tested in the 0.1–1 mM range.

Transmetalation Experiments. The reactions of **G1-4GdDOTAGA** and **G1-4GdDO3A** with Zn^{2+} ions were monitored by measuring the longitudinal relaxation rates R_1 $(1/T_1)$ of water protons on a Bruker mq20 minispec relaxometer (0.47 T), by the inversion recovery method. 12 μL of a 2.5×10^{-1} mol L^{-1} solution of $ZnCl_2$ was added to 300 μL of a phosphate buffered solution (pH 7) of the paramagnetic complex (2.5×10^{-3} mol L^{-1}). The temperature was equilibrated and maintained at 37 °C during the experiments. The mixture was stirred, and the measurements were started immediately and followed during 5 days. The $R_1^P(t)$ relaxation rate was obtained after subtraction of the diamagnetic contribution of the proton water relaxation (0.2826 s^{-1}) from the observed relaxation rate $R_1(t)$.

In Vitro Cytotoxicity Studies. NIH/3T3 (ATCC CRL-1658) cell viability was evaluated with an MTT assay (Sigma-Aldrich) in the presence of **G1-4GdDOTAGA**, **G1-4GdDO3A**, **Na$_2$GdDOTAGA**, and **GdDO3ACOOH**. NIH/3T3 cells were chosen as they are commonly used to screen the toxicity of chemicals[15] and nanomaterials.[16] They are well characterized, uniform, and known to provide reproducible results.[17] NIH/3T3 cells were cultured in Dulbecco's Modified Eagle Medium GlutaMax supplemented with 2 mM L-glutamine, 100 U/mL penicillin, 100 μg/mL streptomycin, and 10% fetal bovine serum and maintained at 37 °C under a humidified

DOI: 10.1021/acs.inorgchem.9b01747
Inorg. Chem. 2019, 58, 12798–12808

Scheme 3. Synthesis of G1-4GdDOTAGA

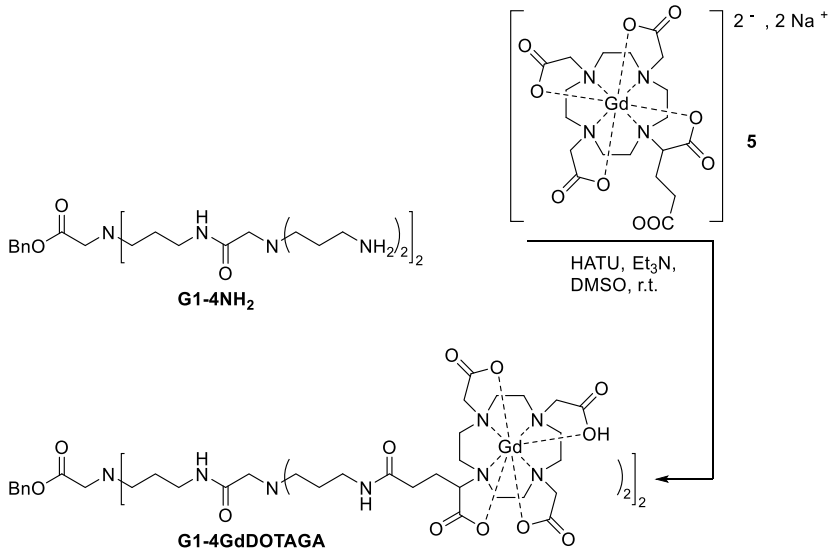

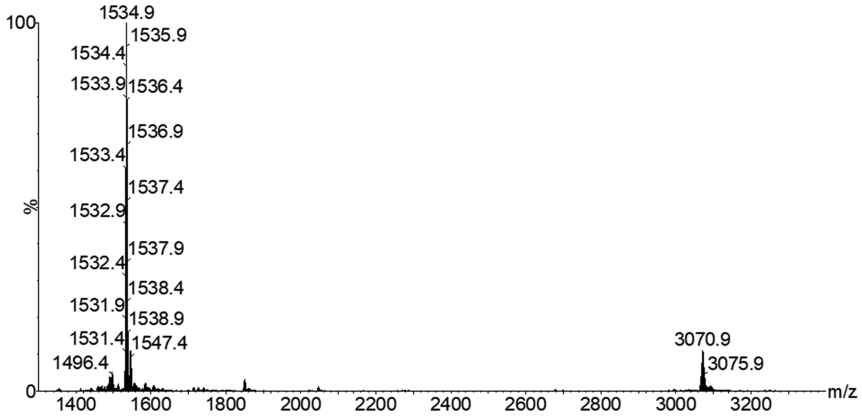

Figure 1. ESI-HRMS spectrum of **G1-4GdDOTAGA** with $[M - H]^-$ and $[M - 2H]^{2-}/2$ signals.

atmosphere containing 5% CO_2. The cells were seeded in a 96 well plate (15.000 cells per well) and were allowed to settle overnight. The next day, **G1-4GdDOTAGA**, **G1-4GdDO3A**, **Na_2GdDOTAGA**, and **GdDO3ACOOH** were added on cells in the following concentrations 0.1, 0.3, 0.5, 0.75, and 1.05 mM of Gd and incubated for 24 h at 37 °C. The medium containing the dendrimers was then removed, and the MTT reagent (100 μL, 1.5 mM in cell medium) was added to each well for 3 h at 37 °C. After taking off the reagents, DMSO was added under shaking for 1 h to dissolve the formazan crystals. The absorbance of each plate was measured at 595 nm with a plate spectrophotometer (PerkinElmer VICTOR^3 1420 Multilabel Counter).

RESULTS AND DISCUSSION

Preparation of G1-4GdDOTAGA and G1-4GdDO3A. *G1-4NH_2 Synthesis.* **G0** (Scheme 2, SI 1, Supporting Information) that will become the core of **G1** dendrimers was synthesized according to a procedure inspired from a published approach,[18,19] where the primary amino groups of 3,3′-iminobis(propylamine) **1** were regioselectively protected by *tert*-butoxycarbonyl groups[20] to give amine **2** (88% yield). Amine **2** was further alkylated with benzylbromoacetate[20] (63% yield) to provide the core structure **G0** with Boc-protected terminal amine functions and a central carboxylic acid function protected by a benzyl (Bn) group. Hydrogenolysis[20] of **G0** gave acid **3** (98% yield) while acidolysis[18] of **G0** gave the bis-amine **4** (92% yield). Acid **3** and amine **4** were then coupled using 2-(1H-benzotriazol-1-yl)-1,1,3,3-tetramethyluronium hexafluorophosphate (TBTU) to give the pentavalent protected dendrimer **G1** (28% yield after silica chromatography). Finally, deprotection of *tert*-butoxycarbonyl groups under acidic conditions afforded dendron **G1-4NH_2** (35% yield).

G1-4GdDOTAGA Synthesis. **G1-4GdDOTAGA** synthesis was achieved from synthon **G1-4NH_2** in the presence of **Gd-DOTAGA 5** (Scheme 3). DOTAGA complexation with Gd_2O_3 afforded complex **5**, and the excess of Gd^{3+} was removed by precipitation after NaOH addition. The peptidic coupling between **5** and **G1-4NH_2** was then performed in the presence of 1-[bis(dimethylamino)methylene]-1H-1,2,3-triazolo[4,5-*b*]pyridinium 3-oxid hexafluorophosphate (HATU). In this approach, the chelate was then metalated before being grafted to the dendron (premetalation strategy).

G1-4GdDOTAGA synthesis was confirmed by means of ESI-MS spectroscopy. The ESI-MS spectrum of **G1-4GdDOTAGA** clearly showed intense signals for molecular ions at $[M - H]^-$ and $[M - 2H]^{2-}/2$, with an isotopically resolved profile matching well with the corresponding simulated signals (Figure 1 and SI 3, Supporting Information).

DOI: 10.1021/acs.inorgchem.9b01747
Inorg. Chem. 2019, 58, 12798−12808

Scheme 4. Synthesis of G1-4GdDO3A

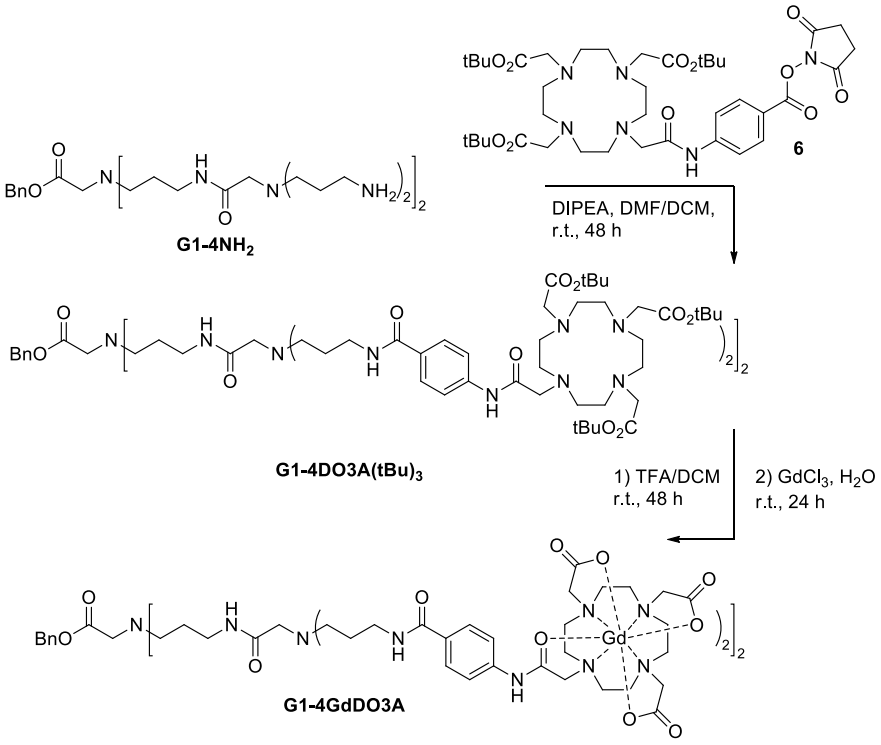

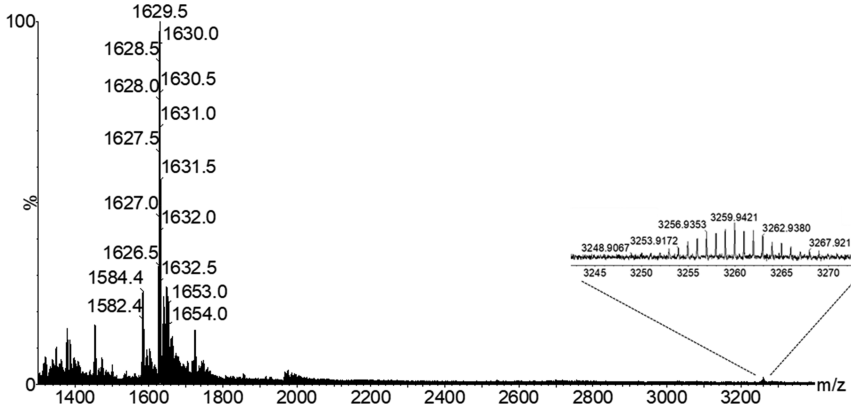

Figure 2. ESI-HRMS spectrum of **G1-4GdDO3A** with $[M - H]^-$ (inset: signal at 3260 m/z) and $[M - 2H]^{2-}/2$ signals.

Therefore, **G1-4GdDOTAGA**, that exhibited 4 Gd^{3+} chelates/per molecule was obtained and readily isolated after ultrafiltration in 73% yield.

***G1-4GdDO3A** Synthesis.* To obtain **G1-4GdDO3A**, a different approach, based on DO3A ligand grafting to **G1-4NH$_2$**, followed by insertion of Gd^{3+} into DO3A chelators of the corresponding dendrimeric ligand, was followed (post-metalation strategy). In a preliminary step, the well-known DO3A-tris-*t*Bu-ester[21] was alkylated with methyl 4-[(bromoacetyl)amino]benzoate. Then the methyl ester group was selectively saponified with lithium hydroxide[22] and the corresponding benzylic acid was treated with EDC and NHS to afford the activated ester **6** (50% yield over 3 steps after a flash chromatography) (SI 4, Supporting Information). The ester **6** was then attached to **G1-4NH$_2$** to provide *t*Bu-protected **G1-4[DO3A(tBu)$_3$]** (Scheme 4). Trifluoroacetolysis of **G1-4[DO3A(tBu)$_3$]** gave **G1-4DO3A** dendron that was finally treated with $GdCl_3$ to afford **G1-4GdDO3A** dendron (9% yield over 3 steps). Excess of Gd^{3+} was removed using a Chelex 100 resin followed by dialysis.

The ESI-MS spectrum of **G1-4GdDO3A** (Figure 2 and SI 5, Supporting Information) clearly showed an intense signal for bis-anionic molecular ion $[M - 2H]^{2-}/2$, with an isotopically resolved profile matching well with its corresponding simulated signals.

To have an insight of **G1-4GdDOTAGA** and **G1-4GdDO3A** hydrodynamic diameters, dynamic light scattering (DLS) was used (SI 7, Supporting Information). DLS analysis indicated Z-ave diameters of 1.70 and 2.50 nm for **G1-4GdDOTAGA** and **G1-4GdDO3A**, respectively. In parallel, DOSY experiments carried out on diamagnetic analogues (G1-4LaDOTAGA and G1-4LaDO3A) revealed hydrodynamic diameters of 2.08 and 1.75 nm, respectively (SI 7, Supporting Information). Given the uncertainties affecting each of these measurements, it can be concluded that the hydrodynamic diameters of **G1-4GdDOTAGA** and **G1-4GdDO3A** were inferior to 2.6 nm.

DOI: 10.1021/acs.inorgchem.9b01747
Inorg. Chem. 2019, 58, 12798−12808

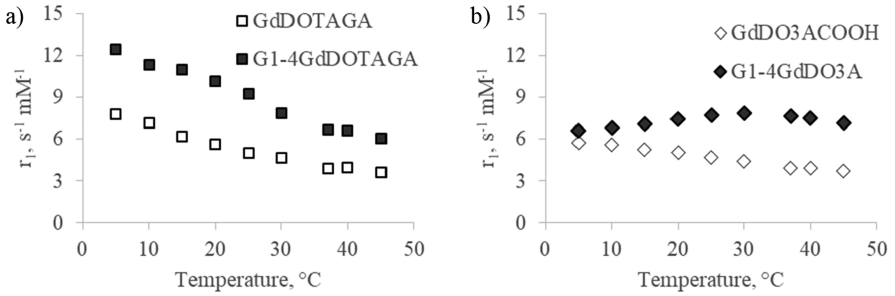

Figure 3. r_1 relaxivity at different temperatures (20 MHz) for (a) **G1-4GdDOTAGA** and (b) **G1-4GdDO3A**.

Finally, to determine the hydration number of Gd^{3+} in **G1-4GdDOTAGA** and **G1-4GdDO3A**, the luminescence lifetimes of the corresponding Eu^{3+} complexes in H_2O and D_2O were measured.[23] τ_{H2O} lifetimes were 0.649 and 0.523 ms for Na_2EuDOTAGA and EuDO3ACOOH, respectively, while τ_{D2O} lifetimes were 2.410 and 1.346 ms, giving a number of water molecules directly coordinated to Eu^{3+} of 1.18 for Na_2EuDOTAGA and 1.23 for EuDO3ACOOH *i.e.* very close to 1 (SI 6, Supporting Information). Assuming the fact that luminescence lifetimes are similar for mononuclear and multimeric complexes, one can conclude that each Gd^{3+} ion in **G1-4GdDOTAGA** and **G1-4GdDO3A** structures exhibited one coordinated water molecule in the inner sphere.

Relaxometric Properties of G1-4GdDOTAGA and G1-4GdDO3A. The proton relaxivity, which describes the MRI efficacy of chelates as contrast agents was first recorded at 20 MHz and 37 °C for both structures. On a per millimolar Gd basis, **G1-4GdDOTAGA** and **G1-4GdDO3A** presented r_1 relaxivities of 6.6 mM^{-1} s^{-1} and 8.1 mM^{-1} s^{-1}, respectively. These values are significantly higher than relaxivities found for the corresponding mononuclear chelates **Na_2GdDOTAGA** and **GdDO3ACO_2H** (3.9 and 4.6 mM^{-1} s^{-1}, respectively), as expected for a longer value of the rotational correlation time associated with the increased molecular size of **G1-4GdDOTAGA** and **G1-4GdDO3A**.[8] In order to characterize the parameters that govern proton relaxivity, r_1 longitudinal relaxivity evolution with the temperature was recorded at 20 MHz for both complexes (Figure 3).

For **G1-4GdDOTAGA**, the continuous decrease of the relaxivity with increasing temperature is characteristic of a fast exchange of the coordinated water molecule in the inner sphere, which means in this case that water exchange will not limit the relaxivity. On the contrary, the observed evolution for the compound **G1-4GdDO3A** is typical of a slower exchange of the coordinated water molecule, limiting the relaxivity. In order to confirm these results and to have an insight into the microscopic parameters governing the dynamics of the system, variable-temperature ^{17}O T_2 measurements were performed to have access to the water exchange rate k_{ex} (equal to the reciprocal lifetime of the water molecule in the inner sphere of the complex, $1/\tau_m$) for **G1-4GdDO3A** and **G1-4GdDOTAGA** (Figure 4).

The observed behavior was completely different for the two complexes and confirmed the results obtained by the evolution of the relaxivity with the temperature. Indeed, a decrease of the transverse relaxation rate was observed with increasing temperature on most of the temperature domain for **G1-4GdDOTAGA**, which is typical of a fast exchange of the coordinated water molecule. The opposite was observed for **G1-4GdDO3A**, indicating a slower exchange of the coordinated water molecule. The experimental data were fitted with a theoretical model as described previously,[14] which allowed extraction of τ_M values of 97 ± 4 ns (k_{ex} = 1.03 × 10^7 s^{-1}) and 505 ± 17 ns (k_{ex} = 1.99 × 10^6 s^{-1}) at 37 °C for **G1-4GdDOTAGA** and **G1-4GdDO3A**, respectively, as well as the thermodynamic parameters governing the exchange (SI 8, Supporting Information). The lower value of k_{ex} obtained for **G1-4GdDO3A** is consistent with data from the literature,[24] where a similar Gd-complex was grafted on a polysaccharide derived from inulin, giving a similar k_{ex} of 1.6 × 10^6 s^{-1}. This difference can be correlated with the structure of the two complexes and more precisely to the functional groups directly coordinated to the Gd center. It is indeed well-known that the presence of an amide group, as in **G1-4GdDO3A**, slows down the exchange of the coordinated water molecule.[25]

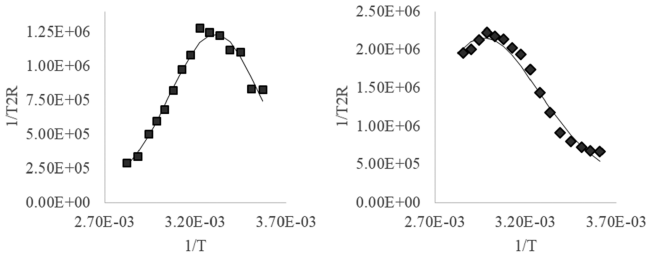

Figure 4. ^{17}O NMR measurements for (a) **G1-4GdDOTAGA** and (b) **G1-4GdDO3A**

Nuclear magnetic relaxation dispersion (NMRD) profiles were also recorded in the field range 0.01−300 MHz for all the complexes.

The **G1-4GdDOTAGA** NMRD profile (Figure 5a) was analyzed using the classical inner sphere and outer sphere theories, which led to a rotational correlation time τ_R of 147.0 ± 2.0 ps (SI 9, Supporting Information), *i.e.* almost two times higher than τ_R of GdDOTAGA (65.1 ± 1.9 ps). This NMRD profile is nevertheless characteristic of a system in a fast rotational motion, which is in relative contradiction with its high molecular weight. When the Lipari−Szabo treatment was incorporated in the fit (Table 1), the order parameter S^2, which describes the degree of spatial restriction of the local rotational motion of the Gd^{3+}-waterproton axis with respect to the global system motion, was almost 0 (S^2 = 0.05), *i.e.* typical of isotropic internal motions. This explains the low value of τ_R extracted from the fitting with the SBM theory.

The **G1-4GdDO3A** NMRD profile (Figure 5b) was analyzed in a similar way, which led to a rotational correlation time τ_R of 242.0 ± 10.0 ps (SI 9, Supporting Information), *i.e.* almost three times higher than τ_R of **GdDO3ACO_2H** (71.2 ± 0.8 ps). The profile exhibited a hump at medium field which is typical of slowly rotating species. When the Lipari−Szabo

DOI: 10.1021/acs.inorgchem.9b01747
Inorg. Chem. 2019, 58, 12798−12808

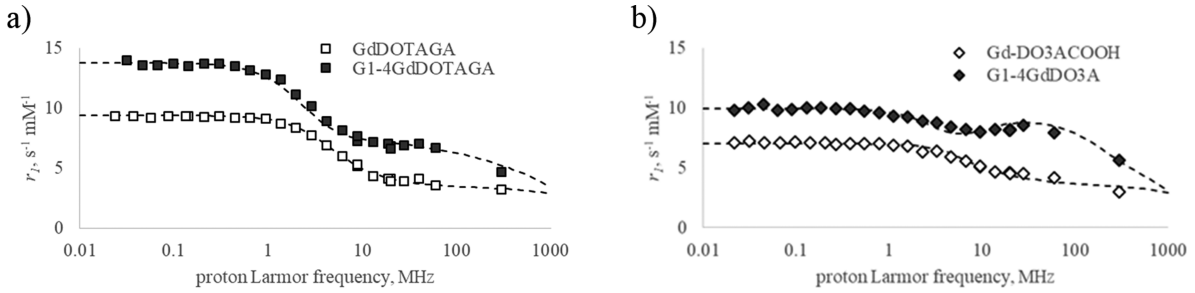

Figure 5. NMRD profiles at 37 °C for (a) **G1-4GdDOTAGA** and (b) **G1-4GdDO3A** (the line represents the least-square fit to the experimental data point as described in the text).

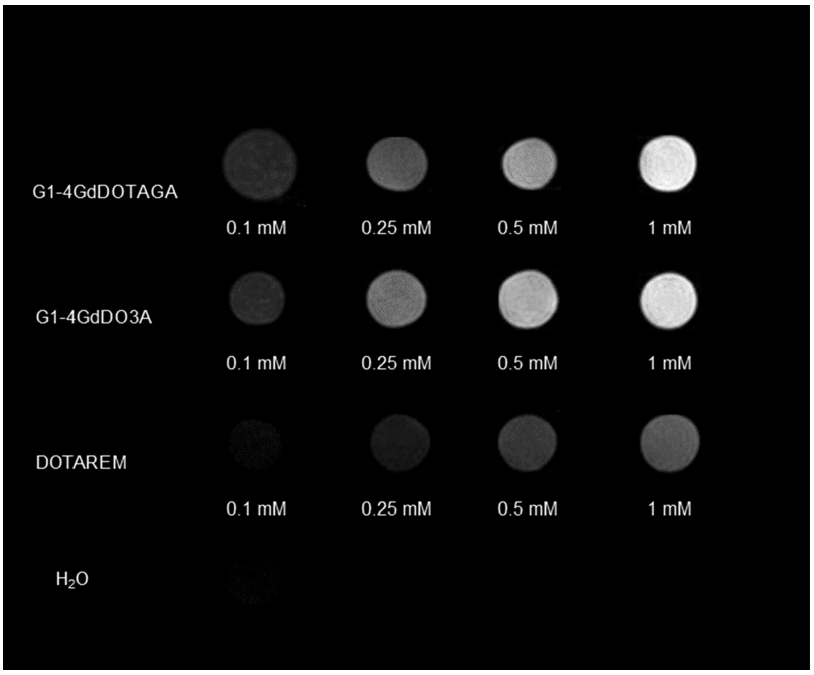

Figure 6. T_1-weighted images of **G1-4GdDOTAGA** and **G1-4GdDO3A** with DOTAREM and water as controls. Samples imaged at 1 T, 37 °C, and with a standard spin echo (SE) sequence.

treatment was incorporated in the fit, the order parameter S^2 was 0.20, which indicated a higher rigidity of this system by comparison to **G1-4GdDOTAGA** (Table 1). This could be correlated with the presence in **G1-4GdDO3A** of the short and rigid aromatic linker,[8e] which was a positive feature to limit the rotation of the small Gd^{3+} chelates. This has thus a positive impact on the relaxivity of this compound, especially at medium field where a hump is observed on the NMRD profile.

To demonstrate how relaxivity enhancements were translated into contrast, T_1-weighted images of phantoms containing solutions of **G1-4GdDOTAGA** and **G1-4GdDO3A** were acquired at 1T with DOTAREM as the control (Figure 6).

For both systems, the bright signal enhancement progressively increased with Gd concentration. Furthermore, for each Gd concentration, **G1-4GdDO3A** or **G1-4GdDOTAGA** signals were brighter than those of the control, corroborating the relaxometric results.

Finally, relaxivity studies of **G1-4GdDOTAGA** and **G1-4GdDO3A** in the presence of human serum albumin (HSA) were performed (Table 2).

G1-4GdDOTAGA demonstrated a very small increase of relaxivity (9%) which could be related to an increase of the medium viscosity. For **G1-4GdDO3A** a more significant difference (49%) was observed, but it is still not high enough to conclude to a noncovalent association to HSA. This should thus allow a fast elimination of the compounds from the body, probably *via* glomerular filtration, given the estimated hydrodynamic diameter of both structures (SI 7, Supporting Information).

Table 2. G1-4GdDOTAGA and G1-4GdDO3A (1 mM, 37 °C, 20 MHz) Relaxivities in the Presence of HSA (4%)

	r_1 (s^{-1} mM^{-1}, H_2O)	r_1 (s^{-1} mM^{-1}, HSA)	$r_1^{HSA}/r_1^{H_2O}$
G1-4GdDOTAGA	6.90	7.50	1.09
G1-4GdDO3A	8.96	13.37	1.49

Kinetic Inertness and Cytotoxicity Evaluations of G1-4GdDOTAGA and G1-4GdDO3A. Before testing **G1-4GdDOTAGA** and **G1-4GdDO3A** safety against cells, their kinetic inertness was evaluated by relaxometry in the presence of Zn^{2+} in a phosphate-buffered solution.[26]

If the transmetalation reaction occurs, it will result in Gd^{3+} release which then will precipitate into $GdPO_4$. Consequently, it will lead to a subsequent decrease of the proton paramagnetic relaxation rate (R_1^P).[26] **G1-4GdDOTAGA** and

DOI: 10.1021/acs.inorgchem.9b01747
Inorg. Chem. 2019, 58, 12798−12808

G1-4GdDO3AR_1^P evolutions gave therefore a good indication of potential transmetalation. Figure 7 showed the evolution of their normalized paramagnetic relaxation rates $R_1^P(t)/R_1^P(0)$.

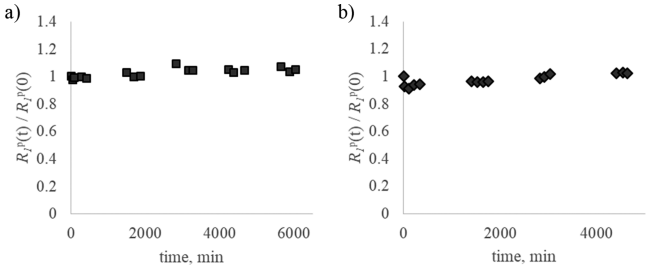

Figure 7. Evolution of $R_1^P(t)/R_1^P(0)$ vs time (at 20 MHz, 37 °C) for (a) **G1-4GdDOTAGA** and (b) **G1-4GdDO3A** in the presence of Zn^{2+} in phosphate buffer (pH = 7)

By comparison to the initial relaxation rate $R_1^P(0)$, no significant changes were observed over a 4 days period for both dendrons, indicating that for **G1-4GdDOTAGA** and **G1-4GdDO3A** no Gd^{3+} release occurred.

G1-4GdDOTAGA and **G1-4GdDO3A** *in vitro* safety was then tested against NIH/3T3 cells (Figure 8).

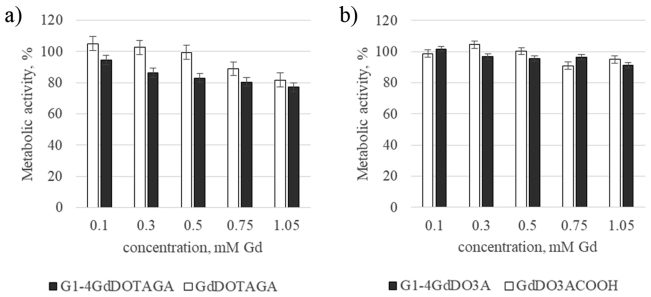

Figure 8. Metabolic activity of fibroblasts (NIH/3T3) incubated with (a) **G1-4GdDOTAGA** and (b) **G1-4GdDO3A** for 24 h (**Na_2GdDOTAGA** and **GdDO3ACOOH** being used respectively as controls).

For **G1-4GdDO3A** no significant decrease in metabolic activity was observed up to a Gd concentration of 1.05 mM (>90% viability for both), and this behavior is similar to that of control. However, a slight and progressive decrease was observed with increasing concentrations of **G1-4GdDOTAGA** to reach 75% at a Gd concentration of 1.05 mM. This follows the same trend as for **Na_2GdDOTAGA** alone, which likely means the decreasing in metabolic activity cannot be totally attributed to the dendrimer. **Na_2GdDOTAGA** is ionic while **GdDO3ACOOH** is neutral which implies differences in osmolarity that can likely explain these discrepancies in toxicity between the two compounds.

CONCLUSION

Two **G1-4GdCA** assemblies containing **GdDOTAGA** and **GdDO3A** units were prepared and subjected to a ^1H and ^{17}O NMR relaxometric investigation. These compounds have similar mass and molecular sizes but differ by the linkers used to graft the chelates to the organic framework. The multimeric nature of **G1-4GdCA** assemblies allowed an increase in molecular size which was translated into a corresponding increase of τ_R and hence of relaxivity (between 70 and 76% over the monomer units). It should be emphasized that the two multimeric systems were characterized by exchange regimes of water molecule not limiting the relaxivity for **G1-4GdDOTAGA** while limiting for **G1-4GdDO3A**, in agreement with the presence of amide groups at the vicinity of the lanthanide ion. Nevertheless, **G1-4GdDOTAGA** exhibited an NMRD profile typical of a system in a fast rotational motion while the **G1-4GdDO3A** NMRD profile was characteristic of a system in a slower rotational motion. The analysis of NMRD profiles by the Lipari−Szabo theory showed for **G1-4GdDOTAGA** a significant limiting role of the local rotational motions of the chelates which resulted in an effective value of τ_R lower than that expected based on molecular dimensions.

On the other hand, the S^2 value determined for **G1-4GdDO3A** suggested a more restricted motion of the chelates located at the periphery of the assembly. This local rigidity was induced by the aromatic linker used to hook the chelate on the organic framework. Therefore, **G1-4GdDO3A** that still exhibits a derivatizable site is a good candidate for the design of targeting paramagnetic probes for molecular imaging or multimodal probes that combine at least two different imaging techniques. Further works are in progress in these two directions.

ASSOCIATED CONTENT

Supporting Information

The Supporting Information is available free of charge on the ACS Publications website at DOI: 10.1021/acs.inorgchem.9b01747.

Experimental details of new compounds' synthesis and analytical data (HR-ESI-MS mass spectra, luminescence lifetime measurements, hydrodynamic diameters, and fitted parameters of ^{17}O and NMRD data) (PDF)

AUTHOR INFORMATION

Corresponding Authors

*E-mail: sophie.laurent@umons.ac.be.
*E-mail: francoise.chuburu@univ-reims.fr.

ORCID

Félix Sauvage: 0000-0002-8065-4439
Cyril Cadiou: 0000-0002-2737-9976
Stefaan De Smedt: 0000-0002-8653-2598
Françoise Chuburu: 0000-0002-4937-173X

Author Contributions

⊥M.N. and V.M. contributed equally. The manuscript was written through contributions of all authors. All authors have given approval to the final version of the manuscript.

Notes

The authors declare no competing financial interest.

ACKNOWLEDGMENTS

The authors would like to thank the "Programme de cooperation transfrontalière Interreg France-Wallonie-Vlaanderen" for funding the "Nanocardio" project (http://nanocardio.eu), the thesis of M. Ndiaye, T Vangijzegem salary, and the postdoctoral fellowships of V. Malytskyi and F. Sauvage. The bioprofiling platform and the Center for Microscopy and Molecular Imaging (CMMI), both supported by the European Regional Development Fund and the Region Wallone, and the PlAneT platform, supported by the European Regional Development Fund and the Region Champagne

DOI: 10.1021/acs.inorgchem.9b01747
Inorg. Chem. 2019, 58, 12798−12808

Ardenne, are thanked. Maité Callewaert (URCA, ICMR 7312) and Claudio Palmieri (Pr P. Duez Laboratory, UMons) are warmly thanked for their help in DLS and ICP-OES experiments, respectively.

REFERENCES

(1) Doan, B.-T.; Meme, S.; Beloeil, J.-C. In *The Chemistry of Contrast Agents in Medical Magnetic Resonance Imaging*, 2nd ed.; Merbach, A., Helm, L.; Toth, E., Eds.; John Wiley and Sons: Chichester, 2013; p 1.
(2) Wahsner, J.; Gale, E. M.; Rodriguez-Rodriguez, A.; Caravan, P. Chemistry of MRI contrast agents: current challenges and new frontiers. *Chem. Rev.* **2019**, *119*, 957−1057.
(3) Yang, C.-T.; Chuang, K.-H. Gd(III) chelates for MRI contrast agents: from high relaxivity to ''smart'', from blood pool to blood-brain barrier permeable. *MedChemComm* **2012**, *3*, 552−565.
(4) Port, M.; Idée, J. M.; Medina, C.; Robic, C.; Sabatou, M.; Corot, C. Efficiency, thermodynamic and kinetic stability of marketed gadolinium chelates and their possible clinical consequences: a critical review. *BioMetals* **2008**, *21*, 469−490.
(5) Idée, J. M.; Port, M.; Medina, C.; Lancelot, E.; Fayoux, E.; Ballet, S.; Corot, C. Possible involvement of gadolinium chelates in the pathophysiology of nephrogenic systemic fibrosis: a critical review. *Toxicology* **2008**, *248*, 77.
(6) (a) Botta, M.; Tei, L. Relaxivity Enhancement in Macromolecular and Nanosized Gd III -Based MRI Contrast Agents. *Eur. J. Inorg. Chem.* **2012**, *2012*, 1945−1960. (b) Bryson, J. M.; Reineke, J. W.; Reineke, T. M. Macromolecular imaging agents containing lanthanides: Can conceptual promise lead to clinical potential? *Macromolecules* **2012**, *45*, 8939−8952. (c) Tang, J.; Sheng, Y.; Hu, H.; Shen, Y. Macromolecular MRI contrast agents: structures, properties and applications. *Prog. Polym. Sci.* **2013**, *38*, 462−502. (d) Zhou, Z.; Qutaish, M.; Han, Z.; Schur, R. M.; Liu, Y.; Wilson, D. L.; Lu, Z.-R. MRI detection of breast cancer micrometastases with a fibronectin-targeting contrast agent. *Nat. Commun.* **2015**, *6*, 7984.
(7) (a) Villaraza, A. J.; Bumb, A.; Brechbiel, M. W. Macromolecules, dendrimers, and nanomaterials in magnetic resonance imaging: the interplay between size, function, and pharmacokinetics. *Chem. Rev.* **2010**, *110*, 2921−2959. (b) Mc Mahon, M.; Bulte, J. W. M. Two decades of dendrimers as versatile MRI agents: a tale with and without metals. *WIREs Nanomed. Nanobiotechnol.* **2018**, *10*, No. e1496.
(8) (a) Bryant, L. H.; Brechbiel, M. W.; Wu, C.; Bulte, J. W. M.; Herynek, V.; Frank, J. A. Synthesis and relaxometry of high-generation (G5, 7, 9, and 10) PAMAM dendrimer-DOTA-gadolinium chelates. *J. Magn. Reson. Imaging* **1999**, *9*, 348−352. (b) Laus, S.; Sour, A.; Ruloff, A.; Toth, E.; Merbach, A. E. Rotational dynamics Account for pH-dependent relaxivities of PAMAM dendrimeric, Gd-based potential MRI contrast agents. *Chem. - Eur. J.* **2005**, *11*, 3064−3076. (c) Lebduskova, P.; Sour, A.; Helm, L.; Toth, E.; Kotek, J.; Lukes, I.; Merbach, A. E. Phosphinic derivative of DTPA conjugated to a G5 PAMAM dendrimer: an ^{17}O and ^{1}H relaxation study of its Gd(III) complex. *Dalton Trans.* **2006**, 3399−3406. (d) Jaszberenyi, Z.; Moriggi, L.; Schmidt, P.; Weidensteiner, C.; Kneuer, R.; Merbach, A. E.; Helm, L.; Toth, E. Physicochemical and MRI characterization of Gd^{3+}-loaded polyamidoamine and hyperbranched dendrimers. *JBIC, J. Biol. Inorg. Chem.* **2007**, *12*, 406−420. (e) Nwe, K.; Bernardo, M.; Regino, C. A. S.; Williams, M.; Brechbiel, M. W. Comparison of MRI properties between derivatized DTPA and DOTA gadolinium-dendrimer conjugates. *Bioorg. Med. Chem.* **2010**, *18*, 5925−5931. (f) Gugliotta, G.; Botta, M.; Tei, L. AAZTA-based bifunctional chelating agents for the synthesis of multimeric/dendrimeric MRI contrast agents. *Org. Biomol. Chem.* **2010**, *8*, 4569−4574. (g) Floyd, W. C.; Klemm, P. J.; Smiles, D. E.; Kohlgruber, A. C.; Pierre, V. C.; Mynar, J. L.; Frechet, J. M. J.; Raymond, K. N. Conjugation effects of various linkers on Gd(III) MRI contrast agents with dendrimers: optimizing the hydroxypyridinonate (HOPO) ligands with nontoxic, degradable esteramide (EA) dendrimers for high relaxivity. *J. Am. Chem. Soc.* **2011**, *133*, 2390−2393. (h) Tei, L.; Gugliotta, G.; Gambino, G.; Fekete, M.; Botta, M. Developing high field MRI contrast agents by tuning the rotational dynamics: bisaqua GdAAZTA-based dendrimers. *Isr. J. Chem.* **2017**, *57*, 887−895. (i) Jin, M.; Zhang, Y.; Gao, G.; Xi, Q.; Yang, Y.; Yan, L.; Zhou, H.; Zhao, Y.; Wu, C.; Wang, L.; Lei, Y.; Yang, W.; Xu, J. MRI Contrast agents based on conjugated polyelectrolytes and dendritic polymers. *Macromol. Rapid Commun.* **2018**, *39*, 1800258.
(9) Fischer, D.; Li, Y.; Barbara Ahlemeyer, B.; Krieglstein, J.; Kissel, T. In vitro cytotoxicity testing of polycations: influence of polymer structure on cell viability and hemolysis. *Biomaterials* **2003**, *24*, 1121−1131.
(10) (a) Verwilst, P.; Park, S.; Yoon, B.; Kim, J. S. Recent advances in Gd-chelate based bimodal optical/MRI contrast agents. *Chem. Soc. Rev.* **2015**, *44*, 1791−1806. (b) Chilla, S. N. M.; Henoumont, C.; Vander Elst, L.; Muller, R. N.; Laurent, S. Importance of DOTA derivatives in bimodal imaging. *Isr. J. Chem.* **2017**, *57*, 800−808. (c) Wu, M.; Shu, J. Multimodal molecular imaging: current status and future directions. *Contrast Media Mol. Imaging* **2018**, 1.
(11) Barge, A.; Cravotto, G.; Gianolio, E.; Fedeli, F. How to determine free Gd and free ligand in solution of Gd chelates. A technical note. *Contrast Media Mol. Imaging* **2006**, *1*, 184−188.
(12) Laurent, S.; Vander Elst, L.; Muller, R. N. Comparative study of the physicochemical properties of six clinical low molecular weight gadolinium contrast agents. *Contrast Media Mol. Imaging* **2006**, *1*, 128−137.
(13) Vander Elst, L.; Sessoye, A.; Laurent, S.; Muller, R. N. Is the theoretical fitting of the proton nuclear magnetic relaxation dispersion (NMRD) curves of paramagnetic complexes improved by independent measurement of their self-diffusion coefficients? *Helv. Chim. Acta* **2005**, *88*, 574−587.
(14) Laurent, S.; Vander Elst, L.; Houze, S.; Guerit, N.; Muller, R. N. Synthesis and characterization of various benzyl diethylenetriamine-pentaacetic acids (dtpa) and their paramagnetic complexes, potential contrast agents for magnetic resonance imaging. *Helv. Chim. Acta* **2000**, *83*, 394−406.
(15) Sahinturk, V.; Kacar, S.; Vejselova, D.; Kutlu, H. M. Synthesis and characterization of various benzyl diethylenetriaminepentaacetic acids (dtpa) and their paramagnetic complexes, potential contrast agents for magnetic resonance imaging. *Toxicol. Ind. Health* **2018**, *34*, 481−489.
(16) Farcal, L.; Torres Andón, F.; Di Cristo, L.; Rotoli, B. M.; Bussolati, O.; Bergamaschi, E.; Mech, A.; Hartmann, N. B.; Rasmussen, K.; Juan Riego-Sintes, J.; Ponti, J.; Kinsner Ovaskainen, A.; Rossi, F.; Oomen, A.; Bos, P.; Chen, R.; Bai, R.; Chen, C.; Rocks, L.; Fulton, N.; Ross, B.; Hutchison, G.; Tran, L.; Mues, S.; Ossig, R.; Schnekenburger, J.; Campagnolo, L.; Vecchione, L.; Pietroiusti, A.; Fadeel, B. Comprehensive in vitro toxicity testing of a panel of representative oxide nanomaterials: first steps towards an intelligent testing strategy. *PLoS One* **2015**, *10*, No. e0127174.
(17) Sambale, F.; Stahl, F.; Rüdinger, F.; Seliktar, D.; Kasper, C.; Bahnemann, D.; Scheper, T. Iterative cellular screening system for nanoparticle safety testing. *J. Nanomater.* **2015**, Article ID 691069 .
(18) Zanini, D.; Roy, R. Novel dendritic N-sialosides: synthesis of glycodendrimers based on a 3,3′-iminobis(propylamine) core. *J. Org. Chem.* **1996**, *61*, 7348−7354.
(19) Zanini, D.; Roy, R. Synthesis of new S-thiosialodendrimers and their binding properties to the sialic acid specific lectin from Limax flavus. *J. Am. Chem. Soc.* **1997**, *117*, 2088−2095.
(20) Ghatnekar, J.; Hägerlöf, M.; Oredsson, S.; Alm, K.; Elmroth, S. K. C.; Persson, T. Construction of polyamine-modified uridine and adenosine derivatives—evaluation of DNA binding capacity and cytotoxicity in vitro. *Bioorg. Med. Chem.* **2007**, *15*, 7426−7344.
(21) Raghunand, N.; Guntle, G. P.; Gokhale, V.; Nichol, G. S.; Mash, E. A.; Jagadish, B. Design, Synthesis, and evaluation of 1,4,7,10-tetraazacyclododecane-1,4,7-triacetic acid derived, redox-sensitive contrast agents for magnetic resonance imaging. *J. Med. Chem.* **2010**, *53*, 6747−6757.
(22) Henderson, B. J.; Carper, D. J.; González-Cestari, T. F.; Yi, B.; Mahasenan, K.; Pavlovicz, R. E.; Dalefield, M. L.; Coleman, R. S.; Li,

DOI: 10.1021/acs.inorgchem.9b01747
Inorg. Chem. 2019, 58, 12798−12808

C.; McKay, D. B. Structure−activity relationship studies of sulfonylpiperazine analogues as novel negative allosteric modulators of human neuronal nicotinic receptors. *J. Med. Chem.* **2011**, *54*, 8681−8692.
(23) Moreau, J.; Guillon, E.; Pierrard, J.-C.; Rimbault, J.; Port, M.; Aplincourt, M. Complexing mechanism of the lanthanide cations Eu^{3+}, Gd^{3+}, and Tb^{3+} with 1,4,7,10-Tetrakis(carboxymethyl)-1,4,7,10-tetraazacyclododecane (dota)—Characterization of three successive complexing phases: study of the thermodynamic and structural properties of the complexes by potentiometry, luminescence spectroscopy, and EXAFS. *Chem. - Eur. J.* **2004**, *10*, 5218−5232.
(24) Granato, L.; Laurent, S.; Vander Elst, L.; Djanasvili, K.; Peters, J. A.; Muller, R. N. The Gd^{3+} complex of 1,4,7,10 tetraazacyclododecane 1,4,7,10 tetraacetic acid mono(p isothiocyanatoanilide) conjugated to inulin: a potential stable macromolecular contrast agent for MRI. *Contrast Media Mol. Imaging* **2011**, *6*, 482−491.
(25) Aime, S.; Barge, A.; Bruce, J. I.; Botta, M.; Howard, J. A. K.; Moloney, J. M.; Parker, D.; de Sousa, A. S.; Woods, M. NMR, relaxometric, and structural studies of the hydration and exchange dynamics of cationic lanthanide complexes of macrocyclic tetraamide ligands. *J. Am. Chem. Soc.* **1999**, *121*, 5762−5771.
(26) Laurent, S.; Vander Elst, L.; Henoumont, C.; Muller, R. N. How to measure the transmetallation of a gadolinium complex. *Contrast Media Mol. Imaging* **2010**, *5*, 305−308.

DOI: 10.1021/acs.inorgchem.9b01747
Inorg. Chem. 2019, 58, 12798−12808